^{53}Mn–^{53}Cr RADIOMETRIC DATING OF SECONDARY CARBONATES IN A HYDRATED ANTARCTIC MICROMETEORITE R. C. Ogliore[1], N. Liu[1], E. Dobrică[2], P. H. Donohue[3], C. E. Jilly-Rehak[4], J. Duprat[5], C. Engrand[5], A. J. Brearley[2]. [1]Department of Physics, Washington University in St. Louis, St. Louis, MO 63130, USA, [2]Department of Earth and Planetary Sciences, University of New Mexico, USA, [3]Hawai'i Institute of Geophysics and Planetology, University of Hawai'i at Mānoa, Honolulu, HI 96822, USA, [4]Space Sciences Laboratory, University of California at Berkeley, Berkeley CA 94720, USA, [5]CSNSM, Univ. Paris Sud, Université Paris-Saclay, 91405 Orsay Campus, France.

Introduction: Hydrated fine-grained Antarctic micrometeorites (H-FgMMs) show general mineralogic similarities to carbonaceous chondrites of petrologic types 1-2, hinting that they may have originated in the same parent bodies. However, our recent work has shown that magnetites in H-FgMMs sampled an O isotope reservoir distinct from that sampled by carbonaceous and ordinary chondrites [1]. One H-FgMM from the Concordia collection, 03-36-46 (Fig. 1: 100 μm, composed of occasional Ca-phosphates, magnetites, and carbonates embedded in homogenous, fine-grained phyllosilicates), contained a magnetite-carbonate assemblage with an inferred precipitation temperature of 160°–280°C (as measured by the oxygen isotope fractionation between carbonate and magnetite) [1], 100°–200°C warmer than the precipitation temperature measured in Al Rais (CR2) [2]. The mineralogy, O isotope composition of magnetites, and inferred precipitation temperature of 03-36-46 do not all match a known meteorite class, implying that 03-36-46 may be from a body not sampled in the meteorite collection.

Recent measurements of the ^{53}Mn–^{53}Cr ($t_{1/2}$=3.7 Myr) system in secondary minerals (carbonates, fayalite, kirschsteinite) from CV, CO, CR, and L chondrites show that these phases mostly formed ∼2–5 Myr after the formation of CV CAIs [3, 4, 5], though calcites from GRO 95577 (CR1) are much younger (11-15 Myr after CAI). If these secondary phases formed by parent-body aqueous processing, accretion of the parent body must have pre-dated the measured ages. Thermal modeling and ^{53}Mn–^{53}Cr measurements constrain the accretion ages of the L, CO and CV chondrite parent bodies to be 1.8–3.0 million years after CV CAI formation [5, 6]. To further investigate aqueous alteration on the 03-36-46 parent body, and to facilitate comparisons between 03-36-46 and O and C chondrites, we measured ^{53}Mn–^{53}Cr isotope systematics in 03-36-46 carbonates.

Methods: Seven dolomite grains in 03-36-46, 1–3 μm in size, lie next to a cluster of framboidal magnetites (Fig. 1b). These dolomites were previously measured by SEM-EDS to contain Mn, but the Mn/Cr ratio could not be accurately measured due their small grain size and nearby Cr-rich materials. Ion probe measurements of the ^{53}Mn–^{53}Cr system in chondrites typically employ a ∼5 μm primary beam for spot analyses (e.g. [3]). The small size of dolomites in 03-36-46 necessitates a smaller primary beam, so we used the NanoSIMS at Washington University with a newly installed Hyperion H201 RF plasma source which can achieve a much smaller primary beam diameter. We used a focused 10 pA primary beam of $^{16}O^-$ to achieve a ∼150 nm spot size on the sample (60 pA was used for presputtering). We used magnetic-field peak jumping to collect $^{50}Cr^+$ (which contained unresolved interferences), $^{52}Cr^+$, $^{43}Ca^+$, and $^{54}Fe^+$ in the first magnetic field setting, then $^{53}Cr^+$, $^{44}Ca^+$, and $^{55}Mn^+$ in the second field. Mass-resolving power was ∼5000 for $^{52}Cr^+$ and $^{53}Cr^+$, sufficient to resolve interferences on these isotopes. We collected scanning ion images for each measured species over raster sizes 1.5×1.5–10×10 μm, and 32×32–128×128 pixels (depending on the raster size). We collected data until ^{44}Ca counts began to decrease significantly, typically 15–60 min.

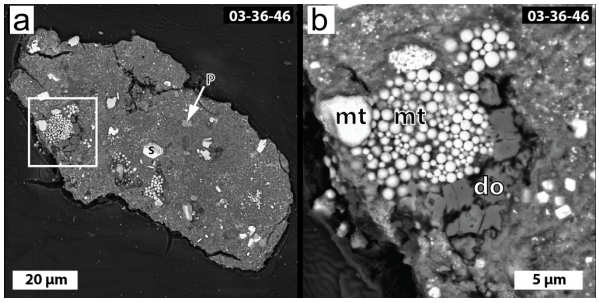

Figure 1: a) Backscattered electron image of 03-36-46 (P=Ca-phosphate, S=sulfide). b) Closer view showing magnetites (mt) and dolomite (do).

We used a synthesized calcite standard with high Mn and Cr concentrations to constrain the Mn/Cr relative sensitivity factor (RSF) of the NanoSIMS. We measured the RSF to be 0.69 in calcite by SEM-EDS (high-precision EPMA work is planned). The RSF for dolomite is typically 20% higher [7], so we assumed an RSF of 0.83 for dolomite.

With this NanoSIMS analytical protocol, we first measured a dolomite grain from Renazzo (CR2), previously measured by [3] to assess the accuracy and precision of our measurement technique.

Data Analysis: We analyzed data using custom Matlab code. We corrected NanoSIMS data for electron-multiplier background counts and deadtime. We aligned the image stacks using the ^{44}Ca channel

then downsampled the images to increase per-pixel statistics. We removed pixels from the edges of each image which are compromised by the crater geometry in the NanoSIMS and other edge effects. We sorted and binnned the pixel data by the ^{55}Mn/^{52}Cr ratio and calculated the ^{53}Cr/^{52}Cr ratio for each bin. We fit a line to these data, while accounting for RSF and different counting times, using a least-squares routine. To calculate uncertainties, we employed a bootstrap approach where we resampled the measured pixels, allowing repeats, and calculated a new linear fit. We repeated this procedure 10^4 times and calculated the standard deviation of the boostrapped distribution for the slope and used this for the standard error of the measured slope. To check the accuracy and precision of our data analysis technique, we substituted artificial Poisson-distributed ^{53}Cr data with a known initial ^{53}Mn/^{55}Mn ratio into our analysis flow. We confirmed that our routine was accurate and reasonably precise, and is not affected by ratio bias [8].

Results: Our measurement of the initial ^{53}Mn/^{55}Mn in one Renazzo dolomite (dol #1) is $(3.7\pm1.4)\times10^{-6}$ (2σ, without RSF uncertainty). This is close in value and precision with $(3.1\pm1.4)\times10^{-6}$ in seven Renazzo dolomites (Figure 2) measured by [3] using spot analyses. Our imaging analysis yields a larger variance in Mn/Cr ratios compared to spot analyses, resulting in a more precise statistical estimate of the isochron slope.

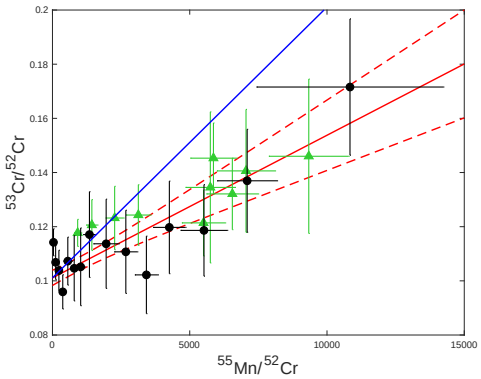

Figure 2: ^{53}Cr/^{52}Cr vs. ^{55}Mn/^{52}Cr for Renazzo dolomite with 2σ error bars (black circles: this work, green triangles: [3]). Red solid line shows our measured slope of 3.7×10^{-7}, red dashed lines show 2σ uncertainty curves, and blue solid line shows a slope of 1×10^{-5} for comparison with Figure 4.

We measured dolomites in AMM 03-36-46 to have Mn/Cr ratios up to only ~200, which is insufficient for precise dating of the ^{53}Mn–^{53}Cr system (Figure 3). Our measured initial ^{53}Mn/^{55}Mn is $(0.06\pm6.5)\times10^{-5}$ (2σ) (Figure 4).

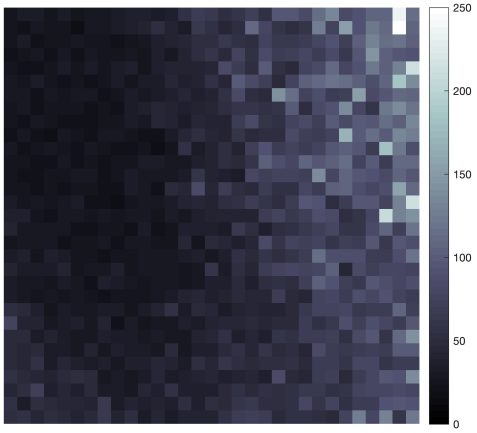

Figure 3: ^{55}Mn/^{52}Cr scanning-ion-image ratio map (1.5×1.5 μm) showing variations at the sub-μm scale.

Conclusions: We developed techniques to accurately and precisely measure the ^{53}Mn–^{53}Cr system in small grains using the Wash U NanoSIMS. We measured this system in dolomites in AMM 03-36-46 but did not find regions with sufficiently high Mn/Cr for a precise measurement. In future work, we will search for carbonates in AMMs and IDPs with Mn/Cr ratios >5000 for NanoSIMS measurements.

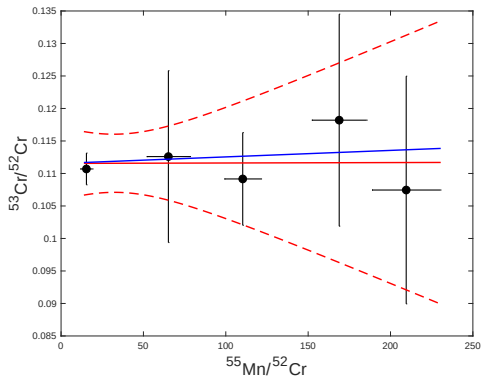

Figure 4: ^{53}Cr/^{52} vs. ^{55}Mn/^{52}Cr for AMM 03-36-46.

Acknowledgements: This work was funded by NASA grant NNH16ZDA001N to E. Dobrică (PI). The micrometeorite collection at the Concordia station was supported by IPEV and PNRA.

References: [1] E Dobrică et al. *LPSC*. Vol. 49. 2018, p. 2666. [2] C. E. Jilly-Rehak et al. *GCA* 222 (2018), 230–252. [3] C. E. Jilly-Rehak, G. R. Huss, and K. Nagashima. *GCA* 201 (2017), 224–244. [4] G. J. MacPherson et al. *GCA* 201 (2017), 260–274. [5] P. M. Doyle et al. *Nat. Commun.* 6 (2015), 7444. [6] N. Sugiura and W. Fujiya. *MAPS* 49.5 (2014), 772–787. [7] K Ichimura and N Sugiura. *LPSC*. Vol. 46. 2015, p. 1795. [8] R. C. Ogliore, G. R. Huss, and K. Nagashima. *NIM-B* 269.17 (2011), 1910–1918.